

CubeSat Mission Concept for Environmental Analysis in Low Earth Orbit

Marco Paolo Brenna^{a*}, Camilla Colombo^{b*}, Francesca Scala^{b*}, Mirko Trisolini^{b*}

^a First author marcopaolo.brenna@mail.polimi.it

^b Co-author camilla.colombo@polimi.it, francesca.l.scala@polimi.it, mirko.trisolini@polimi.it

* Politecnico di Milano, Faculty of Industrial Engineering, Department of Aerospace Science and Technologies, Master in Space Engineering

Abstract

To ensure future space development and sustainable orbital exploitation, it is essential to improve the knowledge of the space environment and of the phenomena that could influence spacecraft's operations. Space debris could pose a threat to space operations, and a collision with such an object could degrade the mission performance. Space debris' environment knowledge is mainly based on ground radar observations, that allow to precisely identify objects of at least 5-10 cm in diameter in Low Earth Orbit. For smaller debris only statistical models on their concentration are available, but these models are affected by uncertainties, due to the scarce amount of data and the difficulty to model and predict space debris evolution. Moreover, the atmospheric models' uncertainties highly affect the end-of-life trajectory changing the ground footprint and the casualty risk. This work addresses the emerging need to characterise the sub-millimetre scale debris environment of the Low Earth Orbit region and to improve models' accuracy during the atmospheric re-entry event of space objects. In this work, a preliminary mission study is proposed to design a 12-unit CubeSat equipped with an array of payloads, selected to characterise the sub-millimetre debris particles and the upper atmosphere temperature and pressure, as well as aerodynamic and thermal loads on the spacecraft. Initially, a parametric orbit selection for the mission is presented. The key parameters were identified as the number of sub-millimetre scale debris' impacts on a sensitive surface of the payload, the residence time of the spacecraft in the upper atmosphere, in particular the region below 200 km altitude, and the compliance with the decay time regulations. A trade-off analysis of possible payload technologies for in-situ detection of sub-millimetre scale debris is presented, starting from state-of-the-art devices. Moreover, the possibility to retrieve re-entry data below 200 km altitude poses a constraint to the residence time below 200 km to be able to collect enough data. Finally, a preliminary design of the CubeSat main subsystems is presented, for an initial definition of mission budgets. This work aims at proposing a feasibility study for a CubeSat mission concept for more sustainable use of space, focusing on space debris and atmospheric modelling.

Keywords: CubeSat, LEO, Space Debris, Reentry analysis, Collision Avoidance, Space Environment

1. Introduction

Since 2015, all United Nations Member States have adopted the 17 Sustainable Development Goals (SDGs) to recognise the vital role of social, economic, and environmental sustainability for the future development of the economy and technology [1]. The protection of Earth's environment, including the atmosphere, forests, oceans, and space, is one of the priorities of the SDGs.

This work aims at improving the knowledge of the Low Earth Orbit (LEO) environment, with a better understanding of the space debris distribution, and more detailed atmosphere and re-entry models. This work proposes an innovative space mission concept, called e.Cube [2], in the field of Space Situational Awareness and Space Traffic Management activities,

for more sustainable and safer access to Space. The e.Cube mission concept focuses on three main objectives [3]:

- i. Characterise the sub-centimetre scale debris environment of the LEO region thanks to in-situ detection.
- ii. Test a new concept of autonomous on-board collision avoidance system.
- iii. Retrieve data during the re-entry phase.

The first two objectives have a complementary purpose: the collision avoidance of traceable debris on one side and the improvement of the damage assessment from untraceable debris on the other. The re-entry analysis aims at reducing the model uncertainties on the post-mission disposal, and

specifically on the re-entry phase, which arise due to the atmospheric modelling (especially the solar activity) and the satellite demise and break-up process, a process for which little to no mission-related data is currently available.

The recent growth of space debris particles is mainly caused by explosions, in space collisions and breakups of space infrastructures, which are the primary source of debris in millimetres and centimetres size. Previous studies have identified the maximum debris concentration altitude in the region between 800 and 1000 km and at about 1400 km [4]. The debris environment characterization is mainly based on ground-based radar and optical measurements that recognize objects as small as 5 cm to 10 cm in LEO. In LEO the United States Space Surveillance Network (US SSN) offers a database for more than 42,000 in-orbit objects [5][6]. For smaller debris only in situ observations during experimental and statistical analysis can provide information and data. The Mid-Course Space Experiment (MSX), launched in 1996, was one of the first satellites to detect space objects. Nevertheless, the optical instruments have a very strong limitation in detecting small particles, with a diameter lower than 1 cm, and the debris population at this level can be represented only via statistical models. Some studies have been done to support the development of particle impact detection technologies, such as DRAGONS [7], and ARMADILLO [8] sensors. The study of space debris provides crucial information for planning space operations and could benefit from innovative debris detection systems for CubeSats, providing in-situ data collection.

Moreover, for debris mitigation purposes, active collision avoidance is becoming a routine task in spacecraft operations. Such an approach requires 27/7 operators' availability, to analyse the parameters and constraints of the conjunction event, with consequently high operational costs. ESA's proposal for a Space Safety Program in 2020 includes a cornerstone "Collision Risk Estimation and Automated Mitigation (CREAM)" [9]. It entails the development of technologies for automating collision avoidance and its demonstration with a suitable newly developed or existing flying platform. New manoeuvre decision criteria and automated approaches should be investigated to face the increasing space traffic management challenge, such as machine learning techniques.

The Inter-Agency Space Debris Coordination Committee (IADC) defined a set of mitigation guidelines, which also served as input to the space debris mitigation guidelines adopted by the United Nations Committee on the Peaceful Uses of Outer Space (UNCOPUOS) [10]. Moreover, to limit the

permanence of man-made objects in orbit after the end of a mission, the space agencies are developing effective Post Mission Disposals (PMD). The adoption of these new technologies to passivate and dispose of missions are expected to limit the growth of space traffic, with advantages in costs operations, collision risks and debris generation. The re-entry phase is a critical part of the mission design because it is influenced by the uncertainties in the atmospheric model, orbital perturbations, and thermomechanical and breakup properties of the spacecraft. The design of atmospheric entry relies on simulation tools, whose models are validated and developed thanks to in-situ measurement or tests inappositely designed facilities, that reproduce the flight environment, such as the Range Safety Assessment Tool (RSAT) [11]. Such analysis is influenced by the presence of high uncertainties in the re-entry event, and it requires in-situ measurement during the re-entry and breaks up of a space object, to validate the data. The Aerospace Corporation, in partnership with NASA's Ames Research Center, has developed a prototype for a new system for collecting and returning data collected in the stressing re-entry environment, the Re-Entry Breakup Recorder (REBR) [12]. A better understanding of the re-entry phenomenon is necessary to improve the guidelines to design missions with the safe end of life de-orbiting. Proper validation and improvement of the currently existing models and tools could enable researchers and engineers to build confidence in the use of these design tools, mature their development, and reduce risk in future heat shield designs.

The aim of the e.Cube mission is to develop three different payloads, to address the mission objectives. First, the spacecraft will mount a payload to collect in-situ data on sub-centimetre scale debris in LEO regions. Moreover, thanks to an on-board algorithm, the satellite will perform autonomous collision avoidance decisions and manoeuvres. Finally, at the end of the mission, a specifically designed payload will retrieve information on the re-entry environment and dynamics.

The paper is organized into eight main sections. Section II describes the mission requirements for the e.Cube spacecraft and section III provides a general overview of the mission architecture and the concept of operations. Section IV describes the scientific payloads chosen to accomplish the mission objectives. The design process of the mission orbit profile is described in section V. Section VI presents an overview of the CubeSat main subsystems and components, while Section VII summarise the mission budgets. Finally, the conclusions are in Section VIII.

2. Mission Requirements

This section provides an overview of the main requirements for the e.Cube mission concept. The main mission requirements are described in Table 1.

The trade-off on the detected debris dimensions is a result of both the need to investigate the sub-centimetre scale debris and the instrument capabilities. It is important to grant the functionality of collision avoidance with different warning scenarios. It is important to perform more than one test, to have enough data to assess the system performance. Typically, a 90% success probability is taken as a satisfying value to be compliant with the guidelines to limit debris growth in LEO [13]. Moreover, the mission shall be compliant with the debris mitigation guidelines. The length of the mission is driven by the necessity to recover a minimum number of debris data.

To accomplish the mission's tasks, the spacecraft is equipped with three different payloads. The decision of a 12 U nanosat was taken after a preliminary mission budget have been evaluated and considering the necessity to equip the spacecraft with 3 different payloads and a propulsion system. The main system requirements are reported in Table 2.

For the autonomous CAM testing phase, the most stringent requirements are on the ADCS and PS subsystems. The optimum collision avoidance manoeuvre is computed on-board, and this shall be done in a reasonable time - about 1 orbit - to allow the manoeuvre to be performed with enough time before the conjunction.

Table 1. e.Cube mission requirements.

MR-01	<i>The debris detection subsystem shall be able to detect debris between 1e-6 m to 1e-3 m</i>
MR-02	<i>The spacecraft shall perform at least 3 collision avoidance demonstration manoeuvres, everyone referring to a different warning time</i>
MR-03	<i>The re-entry analysis shall be performed from 200 km to 100 km altitude</i>
MR-06	<i>The orbit altitude of the satellite shall be between 500 km and 900 km altitude. The orbit shall be a Sun Synchronous orbit</i>
MR-07	<i>The orbit altitude of the satellite shall be chosen to have a minimum number of man-made debris impacts per year of at least 100</i>
MR-08	<i>The mass at launch shall be of maximum 20 Kg</i>
MR-09	<i>The operational lifetime of the mission shall be at least 1 year</i>

Table 2. System requirements.

SR-01	<i>The delta-v budget for the mission shall be at least 150 m/s.</i>
SR-02	<i>The ADCS s/s shall provide at least a 0.07 deg/s slew rate</i>
SR-03	<i>The spacecraft structure shall withstand aerodynamics loads during the re-entry phase.</i>
SR-04	<i>The ADCS s/s shall provide 5° deg of pointing accuracy during the re-entry analysis phase</i>
SR-05	<i>The power consumption of the payload shall be limited to 4000 mW</i>
SR-06	<i>The maximum weight of the payloads shall be 3.5 Kg</i>
SR-07	<i>The maximum space occupied by payload shall be 4 U</i>

During the re-entry phase, the satellite retrieves the data thanks to the re-entry payload, sending them to the ground before the break-up of the spacecraft and the loss of communication possibilities. The attitude control system shall be able to control the attitude of the spacecraft during this phase. To check the atmosphere characteristics, its pressure and temperature will be measured. To reconstruct the break-up process of the spacecraft, both temperature and accelerations on the structure will be measured, to have the thermodynamic behaviour of the spacecraft.

3. Mission architecture and Concept of operations

This section presents the preliminary mission architecture, together with the concept of operations for the mission under analysis.

To accomplish the three mission objectives, the spacecraft will be equipped with three dedicated payloads. Every payload will work in a specific part of the mission, globally called the science phase. For every scientific goal, a trade-off on the possible strategies has been carried out. To satisfy the scientific needs and to fit the payloads and the relative systems inside the spacecraft, a 12-unit CubeSat was selected from the trade-off results on the three payload dimensions and weights.

For the debris analysis, the main driver for the technology selection has been the Technology Readiness Level (TRL) of the payload. Non-impact detectors are still in their development phase, while the impact-based debris payloads have flight heritage, and have proven their effectiveness in many different missions, for example, Cassini or Rosetta missions. An impact detection system has then been chosen for the mission. Possible optical devices with formation flying

instead have been discarded due to high costs, system complexity, and risk.

For the collision avoidance algorithm tests, the strategy chosen is based on a synthetic debris collision message, thanks to its reduced risk and high fidelity compared with a real debris case scenario, which has not been considered for safety reasons.

At the end of the main phase, the deorbit is performed thanks to a multi-impulse manoeuvre, with the aid of a warm gas thruster. The possibility of using solar sails for deorbiting was not considered because of their complexity, the high folding volume required, and higher failure risk. The low thrust electric engine has been evaluated, but the high amount of power needed is not sustainable by the CubeSat without increasing the area of the solar panels with large wings. This would add more stress to the attitude control system, during the re-entry phase. For this reason, the chosen alternative has been the chemical thruster. Both single manoeuvre and multiple manoeuvres have been considered. A trade-off analysis has been performed to both minimise the ΔV for the de-orbit and maximise the time spent in the region between 200 and 100 km altitude. In addition, the risk related to each strategy has been evaluated. To reduce the risk derived by a failure or uncertainties during the firings, the ΔV has been divided into multiple impulses, being able to correct possible errors in the manoeuvres with the subsequent ones.

During the re-entry analysis phase, the spacecraft will collect data thanks to a variety of sensors. These include accelerometers, temperature, and pressure sensors. The CubeSat will then burn in the atmosphere before reaching the ground. The surviving payload has been discarded for excessive dimensions and weight, and the daughter satellite equipped with an optical instrument was not innovative with respect to the previous re-entry observations.

3.1 Concept of Operations

The mission phases are described in Table 3. After the launch phase, the spacecraft starts to activate all its operative systems. In the routine phase the spacecraft carries out the debris analysis, and the on-board autonomous collision avoidance manoeuvre is tested.

The debris analysis will last several months, to collect enough data to allow statistical modelling of the debris environment. At the end of the debris science phase, the spacecraft begins the de-orbiting phase, by lowering the perigee via multiple ΔV at the apogee. After 5 manoeuvres at the apogee, the perigee is lowered to about 200 km altitude. The impulsive manoeuvres are separated about 10 days from one to another, to allow orbit corrections or recalculations if needed. As soon as the spacecraft orbit lower its perigee below 200 km, the re-entry analysis phase starts. The spacecraft permanence under 200 km before the re-entry has been computed to be about 9 days. The orbit lowering continues mainly due to aerodynamic drag. Under 100 km height, the attitude control system is no more able to ensure the control of the spacecraft, and the CubeSat starts decay: the spacecraft will burn up in the atmosphere, below about 80 km of altitude.

4. Scientific Payloads

This section presents the characteristics and the functionalities of the scientific payloads. The instrument's performance has been defined to be compliant with the mission objectives and to be compatible with a 12U CubeSat.

4.1 Debris Analysis Phase

A preliminary study on the payload position has been carried out, considering a 12U CubeSat moving along a Sun-synchronous 800 km orbit, which represent the peak in the debris density distribution with respect to altitude. The sensitive area of the payload is set as 0.04 m², to fit the side face of a 12U CubeSat. The objective of the simulation was to identify the face of the CubeSat with the highest amount of debris impacts. The results show a higher flux in the frontal direction, on the surface positioned toward the velocity direction, which has then been chosen as the target position for the debris detection payload.

An impact detector specifically designed for CubeSats is the piezoelectric detector implemented for the ARMADILLO CubeSat, that can detect sub-millimetre particles [14]. Thanks to its capability to retrieve various information and data, in particular the

Table 3. Preliminary concept of operations

ID	Phase	Description	Duration
1	Launch and Early Orbit Phase (LEOP)	- Launch and Orbit injection - First switch on of the s/c	~ some hours
2	Commissioning Phase	- P/L test and calibration - Platform subsystems check	~ some days
3	Routine phase	3a. Debris Analysis Phase 3b. Autonomous CAM Phase 3c. Re-entry Analysis Phase	~ 8 months ~ some weeks ~ 9 days
4	End of Mission Phase	- s/c decay and burn in the atmosphere	~ hours

debris mass, size and source, and its effectiveness and reliability, ARMADILLO's PDD has been chosen as a baseline payload for the mission. It weighs 393 g for a total volume of fewer than 500 cm³. The required power is 2.98 W, and the estimated data rate is about 150 kB/day. For the mission, the payload is expected to be four times bigger than the baseline payload, thanks to the higher volume and space available on the 12U CubeSat. The expected weight then will be around 1 kg for a volume of 2000 cm³. The sensitive area is 200x200 mm. Also, the power required, and the data rate will be higher, and the expected values are around 500 kB/day and a power budget of 5 W.

4.2 Collision Avoidance Manoeuvre

The collision avoidance manoeuvre payload will implement the algorithm developed at Politecnico di Milano by the COMPASS project [15] to compute via analytic instruments the best collision avoidance manoeuvre directly on-board the satellite. The system will compute the optimum manoeuvre based on risk and propellant cost. It is based on machine learning algorithms, trained on the ground with historical and synthetic CAM datasets. The CAM algorithm is currently at TRL 4. To perform the in-orbit tests a minimum ΔV of 5 m/s has been identified, based on a preliminary analysis made with the DRAMA tool [16].

4.3 Re-entry analysis

The architecture for the re-entry analysis is based on a network of sensors for environmental characterisation, in the altitudes band between 200 km and 100 km. To characterise the re-entry environment and spacecraft response to aerodynamic loads, it is necessary to get information on atmosphere density, aerodynamic loads on the spacecraft and structures heating and internal loads. A preliminary selection of pressure and temperature sensors is given in Table 4. Moreover, the spacecraft is equipped with inertial measurement units based on MEMS technology, to register the re-entry accelerations, combined with temperature sensors and strain gauge to measure internal heat loads and displacements as in Table 4.

Table 4. Re-entry payload characteristics

Instrument	Dimensions [mm]	Power [mw]	Mass [kg]	Range	Performance
Pressure sensor	-	220	0.009	1e-3 – 1e+5 Pa	Accuracy 5%
Temperature sensor	28.5x35.1x0.18	-	0.028	-200° - 150° C	2 sensitivity levels
Inertial sensor	47x39.6x14	500	0.048	-5 – 5 g	0.05° orthogonal alignment error; 6°/hr in-run bias stability; 0.3°/√hr angular random walk; 0.01% non linearity
Overall	95x95x80	5000	≤0.5	-	-

5. Orbit Selection

In this section, insight on the orbit selection and key driving parameters is presented. The analysis considers different indicators to select the orbit profile of the mission and the science phase. The key parameters that drive the choice of the debris science phase are the number of debris particles and their flux that can be detected by the CubeSat, while for the re-entry phase and the re-entry analysis phase the main drivers are compliance with the re-entry guidance for debris mitigation and compliance with re-entry analysis under 200 km of altitude. The focus is to guarantee complete re-entry below six months and at the same time ensure the highest permanence possible of the spacecraft below 200 km. Furthermore, an important driver for the re-entry orbit profile is the minimization of the necessary ΔV .

5.1 Debris analysis phase

For the debris analyses, ESA's MASTER v8.0.2 and DRAMA v3.0.3 have been used. The first analysis performed at the beginning of the selection process is based on debris density as a function of orbit altitude, in the LEO region, for one year period (01/10/2020 to 01/10/2021). The parameters of the simulation are reported in Table 5. The results of the simulation, shown in Fig. 1, highlight a peak of man-made debris density at about 800 km altitude. The highest impact probability corresponds to an orbital altitude of about 800 km. The objective of the study is to identify the orbit inclination ranges that are more subject to debris pollution. Also, the ratio between man-made and natural source debris is considered as an evaluation parameter. The first simulation is performed with MASTER to evaluate the flux distribution for the considered orbital range. MASTER's input, except orbit's height and inclination, are the same for the whole analysis, and are shown in Table 6. The simulation is performed computing the flux on a flat surface with the normal oriented in the velocity direction. For every different altitude considered, inclinations between 0° and 180° deg have been investigated, with a step of 10° deg between them.

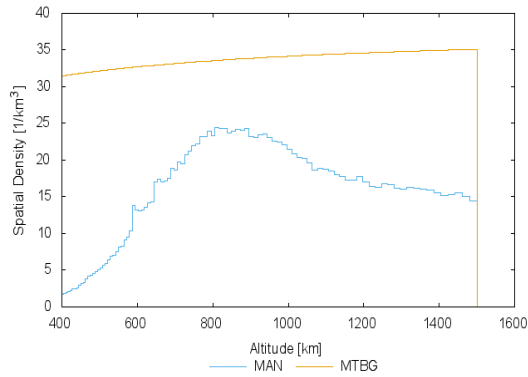


Fig. 1. Debris density vs orbit altitude

Table 5. Input parameters to MASTER for debris density vs altitude analysis.

Parameter	Value
Particle size [m]	1e-6 – 1e-2
Altitude [km]	400 – 1500
Declination [deg]	-90 - 90
RAAN [deg]	-180 - 180
Debris sources	Condensed
Meteoroid sources	Grun

Table 6. Input parameters to MASTER for debris flux analysis.

Parameter	Value
Selection	Earth-bound
Argument of true latitude [deg]	0 - 360
Epoch [y/m/d]	2020/10/1 – 2021/10/1
Eccentricity	0.001
RAAN [deg]	0
Argument of perigee [deg]	0
Resolution [months]	1
Particle size [m]	1e-6 – 1e-2
Debris sources	Condensed
Meteoroid sources	Grun - Taylor
Target surface	Normal direction

At 800 km height, the maximum flux of debris particles is reached. In the orbital planes between 80° deg and 100° deg of inclination, the debris flux value is greater than 100 particles per square metre per year, considering debris bigger than 0.1 mm. The cumulative flux of man-made particles is prevalent on the meteoroid one starting from a dimension of 1e-5 m and reach a value that is more than 2 times higher than it. This is a favourable scenario for the impact detector, which would retrieve a predominant amount of data from man-made objects, with minor influence from the natural dust. Furthermore, in this region are present

“bigger” particles, in the order of 1e-4 m, which study is more interesting from a damage risk assessment viewpoint. This first preliminary analysis on the orbital selection has been done for different altitudes. Moreover, the inclination range among 80° to 110° deg has been identified as the region with higher debris flux per unit surface. Except from 500 km and 550 km orbits, all the analyses identified the maximum in an inclination range comprehensive also of the Sun-synchronous orbit, as shown in Fig. 2. Since these orbits are very busy and of major interest for many missions and many launch opportunities deliver on these orbits, it has been decided to choose a Sun-synchronous orbit as a target for debris analysis.

To refine the analysis in these specific orbits, an impact analysis through DRAMA software has been performed. The MIDAS (MASTER-based Impact Flux and Damage Assessment) tool has been used. The analysis regards the most polluted zones of the previous case study (V.I) and assesses the number of impacts on the sensitive surface of the debris payload, a 20x20 cm. For 600 km the Sun-synchronous orbit inclination is 97.78° deg. This is in the band of maximum debris flux for the region. The previous analysis identified most manmade particles with respect to natural meteoroids, for particles diameters higher than 1e-4 m. In DRAMA analysis this trend is confirmed, and the number of impacts for man-made particles bigger than 1e-5 m is one order of magnitude bigger than the number of the impact of meteoroid sources for most of the sizes. In the upper particles size range, there is a clear distinction between the two fluxes, and a scientific payload that can compute at least the size of the impacting particle can filter the results to have a more precise measurement of man-made debris. At 800 km the peak is reached. The estimated number of detected particles exceeds the 300 units for man-made objects, and it is almost three times the number of meteoroids that would impact the sensitive surface.

The number of particles bigger than 1e-5m increases as well. This is the ideal situation for the science phase, and the Sun-synchronous 98.6° deg 800 km orbit would be the best choice from the debris analysis viewpoint. As a result, from the analyses, the better options in terms of the number of impacts of space debris results in Sun Synchronous Orbits between 800 km to 900 km. However, with different impact levels and characteristics, Sun-synchronous orbits ranging from 550 km to 1200 km can satisfy the requirement of the mission.

For a more immediate comparison between the possible orbits, a comparison between the total number of impacts, due to both man-made, and natural objects and their ratio can be done, as shown in Fig. 2.

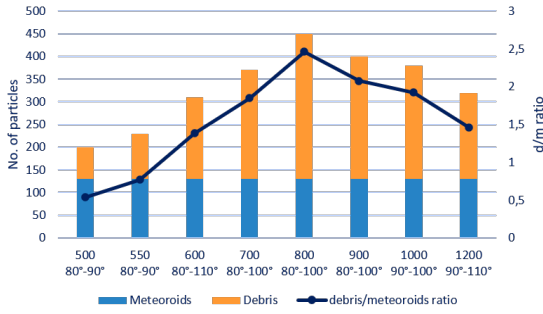


Fig. 2. Impacts per year comparison on the debris sensitive surface (0.04 m²)

The meteoroid flux is constant throughout the region considered; on the other hand, the number of debris impacts ranges from a minimum of 70 impacts at 500 km to a maximum of 320 impacts at 800 km of altitude, for a Sun-synchronous orbit, with the ratio of a man-made/natural particle of 2.46.

5.2 Re-entry analysis phase

The final part of the mission requires a proper manoeuvre to start the re-entry analysis. The reentry payload aims to analyse the atmosphere and its interaction with the satellite in the region between 200 km and 100 km. It is important then that the spacecraft remains in this region for a sufficient amount of time, to allow the payload to collect a satisfying amount of data. To be able to perform the reentry analysis during the mission estimated lifetime of a year and to not exceed the CubeSat lifetime that in general can be assessed to about two years, it is important to guarantee the reentry in at most 6 months. In this way also the ground operations are reduced. The reentry phase should be designed to minimise the required propellant. The analysis is based on the required ΔV . Literature research on off the shelf CubeSat components allows defining an acceptable level of total on board ΔV set around 150 m/s.

The analysis considers a perturbed two-body problem under the effects of the atmospheric drag and Earth gravitational perturbations. The atmosphere density for different altitudes has been computed using an exponential atmospheric model (Eq. 1) [17].

$$\rho(h, t) = \rho_0 e^{\frac{-h+h_0}{H}} \quad (1)$$

For drag computations, the spacecraft parameters taken into account are the cross-sectional area, of 226.3x340.5 mm for a 12 U CubeSat, the spacecraft weight of 10 kg [section VII], and a drag coefficient of 2.2³⁴. The area to mass ratio for the spacecraft is

7.705515e-9 km²/kg. The drag acceleration is then computed as in Eq. 2.

$$\bar{a}_{drag} = -\frac{1}{2} A_m C_d \rho v_{rel}^2 \frac{\bar{v}_{rel}}{\|\bar{v}_{rel}\|} \quad (2)$$

In the model, only the J2 effect has been taken into account, as $J_2 = 0.0010826359$ ³⁴. Mathematically, this is included by expanding the geopotential function at the position (r, Theta, Phi) in a series of spherical harmonics:

$$U(r, \theta, \varphi) = \sum_{n=0}^{\infty} \left(\frac{r}{R_E}\right)^{n+1} J_n P_{n0} \cos \theta + \sum_{n=1}^{\infty} \sum_{m=1}^n \left(\frac{r}{R_E}\right)^{n+1} [C_{nm} \cos m\varphi + S_{nm} \sin m\varphi] P_{nm} \cos \theta \quad (3)$$

The reentry analysis relies on the described orbital model to integrate the perturbed orbit. During the reentry, one or more impulsive manoeuvres are performed to lower the perigee altitude of the spacecraft and reduce the decay time.

5.3 Single impulse manoeuvre analysis

The impulsive manoeuvres are performed at the apogee of the orbit. The required ΔV is computed, and the natural decay begin and last until the stopping conditions for the reentry event function are met; this happens when the spacecraft reaches an altitude of 100 km. The manoeuvres perigee targets are given as an input to the model, which performs the different strategies selected, giving as output the ΔV of every single manoeuvre and the total ΔV for the different strategies. For the last optimisation on the reentry strategy, a genetic algorithm has been used, to optimise the cost function in a predefined range of altitudes targets, as in Eq. 4.

$$J = 0.7\Delta V_{tot} - 3t_{low} \quad (4)$$

The first analysis performed is a parametric study regarding the end-of-life strategy. A first simulation has been performed, considering a single impulsive manoeuvre at the apogee of the operative orbit. The manoeuvre is performed starting from an initial Sun-synchronous circular orbit at different altitudes, ranging from 550 to 1200 km.

These orbits have been chosen according to the considerations done in section V for the debris analysis. The simulation's output is the required ΔV , the total time until reentry and the time spent under 200 km, and are shown in Fig. 3, Fig. 4, Fig. 5, where the y-axis reports the initial altitude, the x-axis the target altitude.

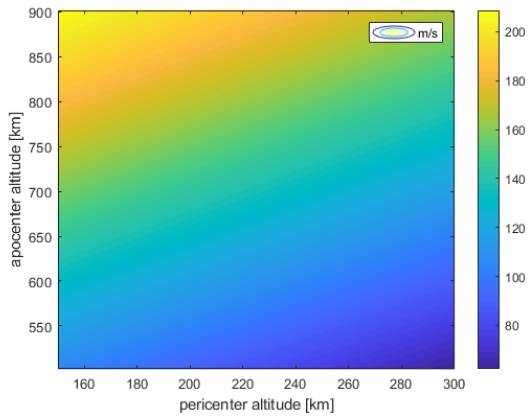


Fig. 3. Single impulse manoeuvre ΔV [m/s] to de-orbit.

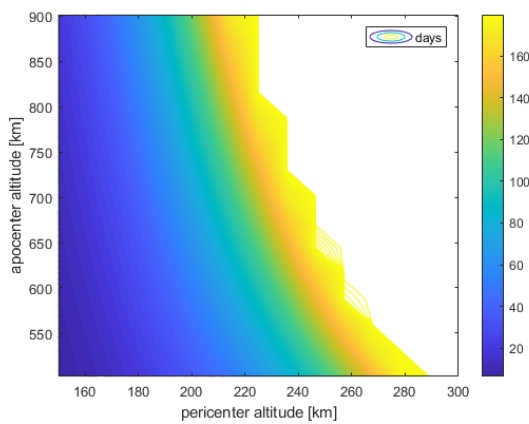


Fig. 4. Number of days before reentry (100 km) for different initial and target altitudes.

Three important considerations can be made:

- To maximise the time spent under 200 km, a final perigee altitude around 200 km shall be targeted.
- No perigee altitudes above 280 km ensure reentry in at least 180 days.
- To have a deorbit ΔV of no more than 150 m/s, no orbit above 900 km altitude can be considered.

5.4 Multiple impulse manoeuvres analysis

The further step in the reentry design is to divide the ΔV in more than 1 firing. For a CubeSat, a multiple

firing ΔV manoeuvre strategy is more conservative and reduces the risk of failures. The first simulation for a multi-impulse reentry strategy has been performed considering 64 different scenarios. The simulation consists of 4 different firings, always at the orbit apogee, starting from 4 different orbit altitudes. From every apogee, the algorithm divides 2 possible perigee altitudes targets for every manoeuvre. In this way, for 4 impulsive manoeuvres, 64 reentry scenarios are created. Between 2 consecutive firings, at least 10 days have to pass, to check the manoeuvre outcome and be able to organize the following manoeuvre if errors in the previous one caused an unexpected orbit track. Furthermore, the waiting time allows exploiting natural perturbances to lower the orbit apogee and reduce the required ΔV . As the first analysis, four different orbit altitudes are considered: 500 km, 635 km, 770 km and 900 km. For every starting altitude, the sub-optimum result is reported in Table 8: Results for different deorbiting strategies for 4 impulses.

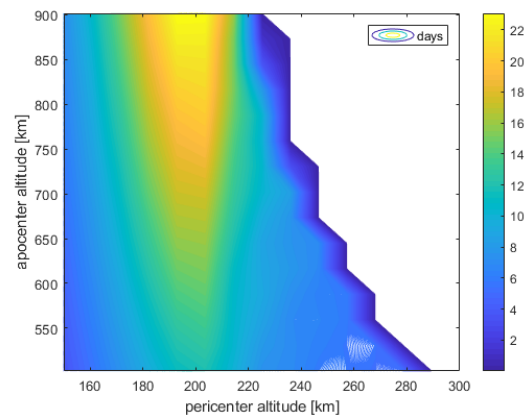


Fig. 5. Number of days spent under 200 km for different initial and target altitudes

To have a total ΔV below 150 m/s, it is necessary to stay in an orbit under 770 km. Furthermore, the best results in terms of the time of flight under 200 km are obtained for the orbits with the lower initial altitudes.

To reduce the effects of a system failure, the chosen orbit shall be chosen to be compliant with the space debris mitigation guidelines even if no propulsion

Table 7. Results for different deorbiting strategies for 4 impulses

H_0 [km]	Steps [km]	ΔV_{tot} [m/s]	ΔV [m/s]	Δt_{tot} [days]	Δt_{200} [days]
500	400-300-200-180	85.05	32.3-27.4-23.5-1.74	61.8	2.09
500	400-350-200-180	85.2	32.3-13.14-38-1.7	61.9	2
635	400-300-200-180	121.8	68.4-27.3-23.8-2.3	63.1	0.23
635	450-300-250-180	121.9	54.4-41.4-9.4-16.9	63.2	0.24
770	400-300-200-180	157.1	103.3-27.3-24.1-2.3	64.3	0.1
770	450-300-250-180	157.2	89.4-41.2-9.7-16.9	64.4	0.08
900	400-300-200-180	191.1	137.1-27.3-24.4-2.3	65.3	0.02
900	450-300-250-180	191.2	123.3-41.2-10-16.8	65.3	0.02

system is available. This corresponds to a natural decay time of 25 years. For a 10 kg spacecraft, the maximum altitude that guarantees a 25 years decay is about 600 km if the best-case scenario is considered [18].

5.5 Orbit profile selection

The final orbit profile of the mission is based on the considerations of both the debris analysis and the reentry analysis and propose a trade-off solution that satisfies mission requirements and at the same time optimise the drivers of the selection. To maximise debris impacts on the detector, the best choice was an orbit between 800 km and 900 km. However, the ΔV required to deorbit from such altitudes exceeds the target ΔV of 150 m/s, and such performance would be a burden for the propulsion system. Furthermore, to ensure a safe mission and compliance with mitigation guidelines, a maximum altitude boundary of 550 km shall be set. From the previous debris impact analysis, in the range between 500 to 600 km, the best option is to choose the maximum value, since higher altitudes are registered with more debris impacts. With these considerations, the operative orbit of the mission is set to 600 km. In Table 7 a summary of the operative orbit parameters is presented.

Table 8. Selected orbit

Parameter	Value
Altitude	600 km
Inclination	Sun Sincronous

To reduce the propellant consumption during reentry and, at the same time, to maximise the time passed under 200 km, and optimisation of the multi impulse strategy has been performed using a genetic algorithm. The function is similar to the previous one: every manoeuvre is performed at apogee, and the time between two consecutive manoeuvres is at least 10 days. The ΔV is given instantaneously, and then the spacecraft follows its natural motion. After further considerations on manoeuvre failure risk, has been decided to add one impulse to the previous 4. The aim is to reduce the first impulse ΔV which was too high for the 600 km orbit. An even distribution of ΔV between the manoeuvres guarantees safer operations and the possibility to recover from a pointing or firing error. The cost function to minimise used for the optimisation is a combination between the total ΔV , expressed in metres per second, and the time passed under 200 km, in days. See equation 4 for details.

The input to the genetic algorithm consists of the range of the target altitudes for the 5 firings. The optimal deorbit strategy starting from a 600 km circular Sun Synchronous orbit is reported in Table 9,

in which the altitude steps and the relative ΔV are reported. The total ΔV for the reentry is 113.08 m/s, and the time spent between 200 and 100 km with this strategy is 8.61 days. The total time elapsed between the first impulsive manoeuvre and the reentry at 100 km in 99.85 days, less than the 180 days decided in the requirements. When all the orbit develops inside 200 km, the altitude continues to decrease due to the action of the drag force, until the boundary line of 100 km is reached and the mission is considered ended. In Fig. 6 the altitude evolution of the reentry after the last firing is shown, and in Fig. 8 an extract of the reentry is presented, focusing on the circularization process that lows the apogee from 600 km down to 200 km and lower. The complete deorbiting phase is shown in Fig. 7.

Table 9. Firing targets and ΔV for reentry phase.

h_a [km]	h_p [km]	ΔV [m/s]
588.34	450.5	36.98
588.1	389.9	14.47
587.3	282.8	34.78
585.3	225.9	20.81
564.1	199.1	6.04

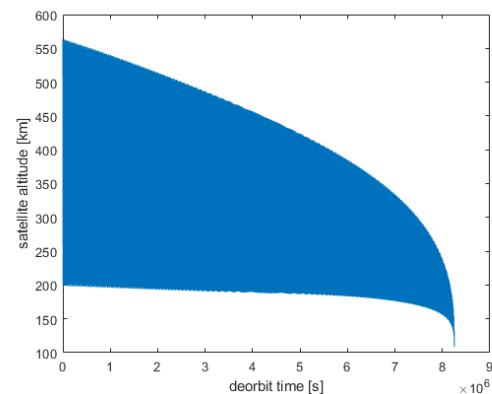


Fig. 6. Spacecraft altitude during reentry.

6. System Design

6.1 Structures

A commercial-off-the-shelf CubeSat structure was considered in the preliminary system design. The 12 U structure of the NPC Spacemind SM12 has been selected as baseline; thanks to its lightweight, only 1750 g with respect to other competitors average of 2 kg, and its versatility in configuration and COTS compatibility. The standard CSD for 12 U satellite allows a maximum spacecraft mass of 24 kg and a size envelope of 23x24x36 cm. This set a constraint on the maximum weight and maximum storage configuration dimensions for the design of the spacecraft.

The preliminary CAD design for the eCube satellite is shown in Fig. 9.

6.2 Propulsion system

The preliminary design of the propulsion system is based on the ΔV budget for the reentry phase, the CAMs and the testing of the autonomous CAM system. The ΔV required for the reentry phase to de-orbit the spacecraft is 135.7 m/s, including a 20% margin [Section V]. The propellant for the collision avoidance manoeuvre has been estimated with the DRAMA ARES tool, considering the baseline orbit selected in Section V. At least 2 collision avoidance manoeuvres are predicted. In the worst-case scenario, a maximum ΔV of 5 m/s is needed. Moreover, it is necessary to add the 5 m/s ΔV required by the testing of the autonomous collision avoidance system. The ΔV budget is then reported in Table 10.

To avoid adding complexity to the attitude control system, the maximum thrust for the on-board engine should not be higher than 1 N. Possible options are a mono-propellant Ammonium Dinitramide (ADN)-based motor of NanoAvionics, and a bipropellant engine of DawnAerospace.

Table 10. Preliminary ΔV budget

Phase	ΔV [m/s]	20% margin ΔV [m/s]
Reentry	113.08	135.7
CAM	5	6
Autonomous CAM testing	5	6
Total	123.08	147.7

6.3 Attitude determination and control system

The attitude determination and control system should be able to keep the velocity pointing of the spacecraft during the science phase with a required accuracy of 1° deg and to guarantee a quick 90° deg slew manoeuvre to ensure collision avoidance capability even if a radial firing is needed. The minimum slew velocity for the aim is set to obtain the 90° deg slew in at least one-quarter of orbit revolution. During the re-entry, the spacecraft should not tumble and it should keep a velocity pointing attitude to perform the reentry analysis phase [19].

The attitude component selection takes as a baseline the attitude control system of ARMADILLO adapting it to the performance demand of a 12 U satellite, which has higher inertia, and a peculiar reentry environment. The system utilizes a set of 3 gyroscopes, two sun sensors, and a magnetometer for basic attitude determination. An external star tracker provides a more accurate attitude determination. A set of three reaction wheels is used for three-axis attitude control of the spacecraft. As for attitude sensors, a preliminary selection of three to six sun sensors, placed on different faces has been chosen.

Two-star trackers are selected for redundancy, together with three gyroscopes, one for every axis for angular velocity measurement, and a magnetometer to measure Earth magnetic field in body axes. A preliminary selection of possible off the shelf components is presented in Table 11. The combination of sensors proposed is compliant with the pointing requirement accuracy for attitude determination. To control the spacecraft, a set of 4 reaction wheels has been considered, disposed of one along each axis and one redundant wheel in the bisector of the three axes. For wheels desaturation and spacecraft detumbling during LEOP, a set of two orthogonal magnetorquers and a cold gas thruster on the spare axis have been considered. For the actuators, a proposed selection of instruments is presented in Table 12.

For the preliminary design, the CubeSat has been modelled as a parallelepiped with dimensions equal to the structural ones. The total weight of the spacecraft has been assumed as 10 kg. The inertia matrix has been computed considering a uniform mass density inside the spacecraft, and it is equal to:

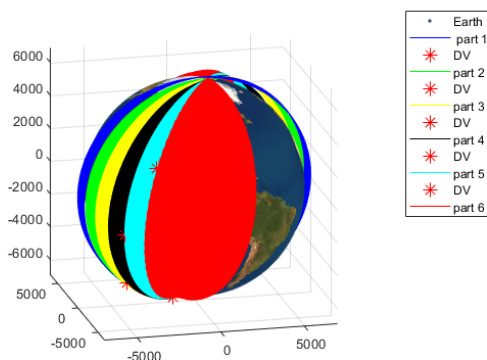


Fig. 7. Reentry phase profile. Blue: operational orbit. Green, yellow, black, cyan, and red: sequence of thruster firings.

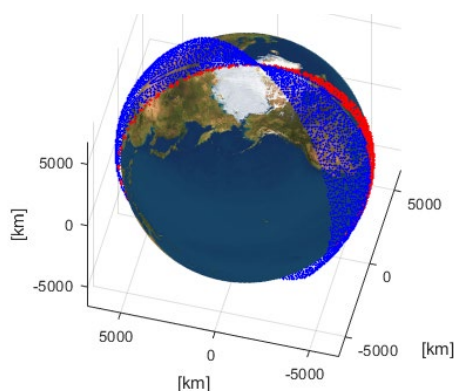


Fig. 8. Natural decay of the orbit after the last manoeuvre. The blue part identifies the altitudes above 200 km, the red part the altitudes under 200 km

Table 11. Sensors selection for attitude determination system.

Sensor	Dimensions [mm]	Mass [g]	Power [mW]	performance
Sun Sensor	33x11x6	5	10	update rate: ≤10 Hz ; ≥0.5° deg RMS error over FOV
Star tracker	50x50x83	106	670	slew rate: 1°/s ; update rate: 5Hz ; accuracy pitch/yaw: 10 arcsec, roll: 70 arcsec
Gyroscopes	38.6x44.75x20	55	1500	125-1000 samples/s; ARW 0.15; customisable filter on every axis
Magnetometer	99x43x17	85	750	update rate: ≥18 Hz; ≥8nT noise density

Table 12. Actuators selection for the attitude control system.

Parameter	iMTQ (magnetorquer)	NanoTorque GSW-600
Mass [g]	196	940
Dimensions [mm]	95.9x90x17	95x95x61.6
Power [mW]	1200	2500 x wheel
Torque	Max dipole moment 0.2 Am ²	Max torque 1.5 mNm
Accuracy	Actuation envelope error ≥5%	Accuracy 0.5 rpm
Characteristics	2 torque rod + 1 air core torquer	max momentum storage 19 mNm/s; max wheel speed 6000 rpm
Company	ISIS	GOMspace

$$I = \begin{bmatrix} 0.1434 & 0 & 0 \\ 0 & 0.1434 & 0 \\ 0 & 0 & 0.08789 \end{bmatrix} \text{kgm}^2 \quad (5)$$

6.4 Position and Orbit Determination and Control

Two GPS receivers are suggested, with related receiving patch antennas, and for redundancy two are then mounted. Possible selections for the GNSS transceivers and antenna components are listed in Table 13; they all work with data from both GPS constellation and GALILEO constellation, and the LEO accuracy satisfies the mission requirements for CAM and reentry analysis phases. For orbital control, there are two alternatives: using the CAM engine to perform also orbital control manoeuvres but can result in poor manoeuvre efficiency [20]; use a dedicated propulsion system, like the one in Table 13, made by

6.5 Command and Data Handling

The component selection suggested in Table 14 refers to a very preliminary data budget assessment. The ARMADILLO payload has been taken as a baseline for this preliminary analysis. It uses as a microprocessor the Phytex phyCORE-LPC3250 SOM (System on a Module), and a 2 SD memory card to collect payload data.

6.6 Telemetry, Tracking and Command

As a baseline, the TT&C architecture from a similar CubeSat mission has been identified. The most demanding phase of the mission from the data rate viewpoint is the reentry phase. During the re-entry phase, the link time between the ground station and the

Table 13. PODC hardware selection

Instrument	Mass [kg], dimensions[mm]	Power [mW]	Properties
GNSS receiver	0.003, 20x14.5x3.1	165	accuracy: 8m, TBD m/s; GPS+GAL
GNSS receiver	0.09, 92x87x12	500	accuracy: 5m, 0.1 m/s, 100 nanosec; GPS+GLO+GAL
Patch antenna	0.018, 70x70x15	48	peak gain: 5.5 dBi; signal gain up to 32.5 dB; GPS+GAL
Patch antenna	0.089, 74x74x13	110	SNR: 50; GPS+GLO+GAL
Monopropellant Propulsion Module	1010, 100x100x100	22000	liquid green propellant ; 0.1-1 N thrust; 224 Isp; 59 m/s ΔV

multiple thrusters.

Table 14. C&DH hardware selection.

Parameter	IMT-OBC	iOBC
Mass [g]	38	76
Dimensions [mm]	96x90x10	96x90x12.4
Power [mW]	300	400
Characteristics	200 MHz; freeRTOS (other option on demand)	400 MHz; freeRTOS or KubOS Linux
Memory	16 MB RAM (64 MB available); 64 MB Flash NOR memory; 8 GB Flash NAND memory	64 MB SDRAM; 1 MB code storage; 256 kB critical data storage; 2 SD cards data storage
Company	IMT	ISIS

Table 15. TT&C hardware selection.

Instrument	Mass [kg], dimensions [mm]	Power [mW]	Properties
UHF/VHF transceiver	0.075, 90x96x15	480-4000	TX: 435-438 MHz or 400.15-402 MHz; other ranges on request; RX: 145.8-146 MHz and 148-105.05 MHz; 9.6 Kbps
X-band transceiver	0.2, 90x65x28	15000	TX: 8025-8500 MHz; RX: 7145-7250 MHz; downlink 25+ Mbps; uplink: 64+ Kbps
UHF Antenna	0.085, -	-	Omnidirectional; 435-438 MHz
X-band patch antenna	0.0022, -	Output power 4000	Gain: 6dB; HPBW: 74° deg; 8025-8400 MHz
4x4X-band patch antenna	0.053, -	Output power 4000	8025-8400 MHz; HPBW: 18° deg; gain: 16 dB
X-band antenna	0.065, 72.6x72.6x11	3000	8025-8400 MHz; HPBW 40° deg; gain: 11.5 dB

Table 16. EPS hardware selection.

Instrument	Mass [kg], dimensions [mm]	Capacity [Wh]	Properties
Battery pack	0.5, 93x86x41	77	Li-ion; autonomous heater; 33.6 V
Power Unit	0.191, 90x96x12.3	-	1 motherboard, 1 ACU, 1 PDU; 3 configurable output voltages; current and voltage measurement

CubeSat shall be carefully analysed. Furthermore, the high temperatures generated by the reentry in the atmosphere and the ionised gases could affect the communication with errors. To be sure to download the necessary data in a short period, transmissions in the Xband are considered [21], to improve the data transmission in a short time. The baseline transmitter, as in Table 15, can have a link rate up to 100 Mbps. The spacecraft is also equipped with a VHF/UHF transceiver, for telemetry, tracking and low power consumption communications.

6.7 Electric power system

Electric power is produced with a set of solar panels. The peak power requested by the spacecraft occurs during CAM phase, and it is about 50 W. To satisfy such a request, by considering a cell efficiency

of 30%, a cell area of 0.123 m² is needed. This would be possible only if deployable solar panels are used. If only body-mounted solar panels are used, considering for example the Azur space solar cells, and two sides of the spacecraft equipped with 16 cells per side, having each cell up to 1.15 W of peak power the resulting peak power generation for perpendicular Sun incidence on the panels would be of 36.8 W. If a 45° deg incidence angle with Sun is assumed, the power generated reduces to 26.02 W [22]. To cover for peak power, a battery pack would be used.

During the CAM, which is the most demanding phase of the mission from the power point of view, is about 23.31 W. Considering 20 minutes of manoeuvre duration, a 1.2 battery conversion factor the capacity used from the battery is 9.32 Wh. Considering a typical

value of 15% of the depth of discharge, the capacity required from the batteries results in 62.26 Wh.

A suggestion on the battery pack selection is the NanoPower BPX from GOMspace, which has a capacity of 77 Wh. Furthermore, it can be matched to the GOMspace NanoPower P60 system; the complete system contains a P60 Dock motherboard and a combination of an Array Conditioning Unit (ACU) and Power Distribution Unit (PDU) daughterboards. The properties of EPS hardware are reported in Table 16.

7. Mission Budgets

A preliminary mass, power and ΔV budget has been assessed for the mission concept. The target was to achieve a maximum of 150 m/s of required ΔV , and the computed marginalized ΔV is 147.7 m/s. The initial power estimated takes as reference an average of 50 W. The driving parameter is to have a power budget that minimises deployable solar panels area.

7.1 Mass budget

In Table 17, the total mass of the subsystem components previously presented, and the marginalised values are reported.

Table 17. Mission preliminary mass budget

Subsystem	Total mass [g]	Total mass with 20% margin [g]
STR	1750	2100
PS	1410	1692
ADCS	1392	1670.4
PODC	116	139.2
C&DH	76	91.2
TT&C	413	495.6
EPS	691	829.2
Payload	1008	1209.9
Total	6856	8227.5

Table 18. Preliminary power budget.

Subsystem	Debris phase [mW]	science	Telecom [mW]	CAM and propulsion [mW]	Reentry analysis [mW]
STR	-	-	-	-	-
PS	-	-	-	15000	-
ADCS	16968	-	16968	16968	16968
PODC	789.6	-	789.6	789.6	789.6
C&DH	480	-	480	480	480
TT&C	-	-	27600	-	-
EPS	294	-	294	294	294
Debris detection payload	3600	-	-	-	-
Autonomous CAM	-	-	-	480	-
Reentry analysis payload	-	-	-	-	6000
Total	22131.6	-	46131.6	34011.6	24531.6

7.2 Power budget

To determine the power required during the different mission phases, the subsystems are then divided into 4 groups, each one representing 1 of the 4 main operations of the mission, as reported in Table 18. The result of the analysis shows that the power request is lower than 50 W in every mission phase.

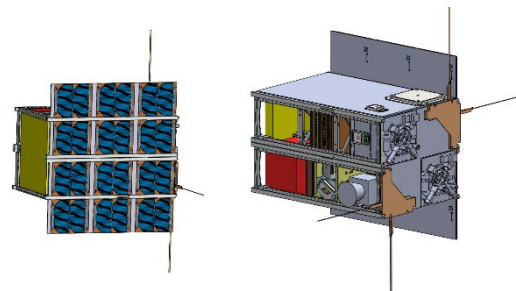


Fig. 9: Preliminary CAD design of the eCube mission.

8. Conclusions

This work demonstrates the feasibility of a CubeSat mission for Low Earth Orbit environment analysis. In particular, the capabilities of CubeSats to characterize the submillimetre debris environment has been investigated. Broad use of CubeSats missions equipped with debris detection payloads could help to improve our knowledge of the orbit environment keeping it cost-effective. Furthermore, it has been presented a CubeSat concept for an in-situ reentry analysis.

The results of such a mission would be valuable to improve the reentry models that nowadays are characterized by high uncertainties. CubeSats have great potential for both science and commercial missions, reducing the costs and improving at the same time the compliance with space sustainability guidelines. The LEO environment characterisation coming from the data analysis of the debris detection

payload and the reentry analysis payload could constitute an important contribution for a better knowledge of the space environment, providing high fidelity models of space debris distribution and atmospheric reentry loads. Moreover, the selection of small thrust propulsion is effective on CubeSats, but future drag augmentation devices could ensure fast reentry with no propellant needed. CubeSats represent a great opportunity to expand a sustainable and wise

use of space and space science, widening the stakeholders pool reducing operation costs and giving standard components to rely on.

References

- [1] Griggs, D., Stafford-Smith, M., Gaffney, O., Rockström, J., Öhman, M. C., Shyamsundar, P., et al. (2013). Sustainable development goals for people and planet. *Nature*, 495(7441), 305-307.
- [2] Colombo, C., Trisolini, M., Scala, F., Brenna, M. P., Gonzalo Gómez, J. L., Antonetti, S., et al. (2021). e. Cube mission: the environmental CubeSat. In 8th European Conference on Space Debris, ESA/ESOC (pp. 1-9). ESA.
- [3] Colombo, C., Scala, F., Trisolini, M., Gonzalo Gómez, J. L., Antonetti, S., et al. (2021). The environmental Cubesat mission e.Cube for low Earth orbit data acquisition. In XXVI International Congress (AIDAA) (pp. 1-6). Pisa, Italy.
- [4] Nazarenko, A. I. (2014). Prediction of the space debris spatial distribution on the basis of the evolution equations. *Acta Astronautica*, 100, 47-56. doi:10.1016/j.actaastro.2014.02.023.
- [5] Majorova, V. I., Leonov, V. V., & Grishko, D. A. (2016). Analysis of approaches to the near-Earth orbit cleanup from space debris of the size below 10 cm. *Aerospace Scientific Journal*, 14-26. 16. doi:10.7463/aersp.0116.0833914.
- [6] Shepherd, L. C. G., & Command, A. F. S. (2006, September). Space surveillance network. In Shared Space Situational Awareness Conference, Colorado Springs, CO.
- [7] Ramsey, M., Ash, D., Bowen, J., Sadilek, A., Bunker, E., Harden, B., et al. (2011). Debris Resistive Acoustic Grid Orbital Navy Sensor (DRAGONS). In Infotech@ Aerospace 2011 (p. 1600). doi:10.2514/6.2011-1600.
- [8] Brumbaugh, K. M., Kjellberg, H. C., Glenn Lightsey, E., Wolf, A., & Laufer, R. (2012). In-situ sub-millimeter space debris detection using cubesats. *Advances in the Astronautical Sciences*, 144, 789-803.
- [9] Flohrer, T., Krag, H., Merz, K., & Lemmens, S. (2019, September). CREAM-ESA's Proposal for Collision Risk Estimation and Automated Mitigation. In Proceedings of the Advanced Maui Optical and Space Surveillance Technologies Conference (AMOS).
- [10] Mejía-Kaiser, M. (2020). iadc Space Debris Mitigation Guidelines. In *The Geostationary Ring* (pp. 381-389). Brill Nijhoff. doi:10.1163/9789004411029_014.
- [11] Capristan, F. M., & Alonso, J. J. (2014). Range Safety Assessment Tool (RSAT): An analysis environment for safety assessment of launch and reentry vehicles. In 52nd Aerospace Sciences Meeting (p. 0304).
- [12] Ailor, W., Dupzyk, I., Shepard, J., & Newfield, M. (2007). REBR: An Innovative, Cost-Effective System for Return of Reentry Data. In AIAA SPACE 2007 Conference & Exposition (p. 6222). doi:10.2514/6.2007-6222.
- [13] United Nations Office for Outer Space Affairs. (2010). Space Debris Mitigation Guidelines of the Committee on the Peaceful Uses of Outer Space. URL https://www.unoosa.org/pdf/publications/st_spac_e_49E.pdf
- [14] Brumbaugh, K. M., Kjellberg, H. C., Glenn Lightsey, E., Wolf, A., & Laufer, R. (2012). In-situ sub-millimeter space debris detection using cubesats. *Advances in the Astronautical Sciences*, 144, 789-803.
- [15] Gonzalo Gómez, J. L., & Colombo, C. (2020). Collision avoidance algorithms for Space Traffic Management applications. In 71st International Astronautical Congress (IAC 2020) (pp. 1-9).
- [16] Brenna, M. P. (2020). CubeSat mission design for in-orbit environment characterisation. Politecnico di Milano, Faculty of Industrial Engineering, Department of Aerospace Science and Technologies, Master in Space Engineering.
- [17] Wertz, J. R., Everett, D. F., & Puschell, J. J. (2011). *Space mission engineering: the new SMAD*. Microcosm Press.
- [18] Brito, T. P., Celestino, C. C., & Moraes, R. V. (2015, September). Study of the decay time of a CubeSat type satellite considering perturbations due to the Earth's oblateness and atmospheric drag. In *Journal of Physics: Conference Series* (Vol. 641, No. 1, p. 012026). IOP Publishing. doi:10.1088/1742-6596/641/1/012026.
- [19] Scala, F., Trisolini, M., & Colombo, C. (2021). Attitude control of the disposal phase of the eCube mission for atmospheric data acquisition. In *SpaceOps 2021 Virtual Edition* (pp. 1-17).

- [20] Ranjan, R., Chou, S. K., Riaz, F., & Karthikeyan, K. (2017). Cold gas micro propulsion development for satellite application. Energy Procedia, 143, 754-761. doi:10.1016/j.egypro.2017.12.758.
- [21] U. D. o. C. Ntia, Manual of Regulations and Procedures for Federal Radio Frequency Channels (2009).
- [22] J. Wertz, D. Everett, J. Puschell, Space mission engineering : the new smad, 2011.